ELSEVIER

E≋RS

Sol–gel synthesis and characterization of Co-doped LSGM perovskites

Riccardo Polini *, Alessia Falsetti, Enrico Traversa

Dipartimento di Scienze e Tecnologie Chimiche, Università degli Studi di Roma Tor Vergata, Via della Ricerca Scientifica, 00133 Roma, Italy

Available online 31 March 2005

Abstract

One of the major requirements for the development and commercialization of low-cost SOFCs is the reduction in the operating temperature. One of the methods to reach this aim is the use of solid electrolytes which exhibit superior ionic conductivity at intermediate temperatures (IT, $T < 800\,°C$). Among these ionic conductors, doped $LaGaO_3$ materials show high oxide ionic conductivity in the 600–800 °C range. These perovskites are usually prepared by time- and energy-consuming solid state reaction. In this paper, $La_{0.8}Sr_{0.2}Ga_{0.8}Mg_{0.2}O_{2.8}$ (LSGM) and $La_{0.8}Sr_{0.20}Ga_{0.8}Mg_{0.2-x}Co_xO_{3-\delta}$ (LSGMC) powders containing different amounts of Co ($x = 0.05$, 0.085 and 0.10) were prepared from precursors synthesised by citrate sol–gel method. The precursors were calcined at 1000 °C (10 h) and dense high-purity pellets were obtained by pressing (300 MPa) and sintering in air at 1475 °C (5, 10 and 20 h). Sintered pellets of LSGM and LSGMC contained very small amounts (<1%) of $SrLaGa_3O_7$ and $SrLaGaO_4$, respectively, as detected by X-ray diffraction (XRD) and by the combined use of scanning electron microscopy (SEM) and energy dispersive spectroscopy (EDS). The data clearly showed the feasibility of sol–gel methods to produce Co-doped LSGM perovskite type oxides.
© 2005 Elsevier Ltd. All rights reserved.

Keywords: Powders–chemical preparation; Sol–gel processes; Sintering; Fuel cells; Perovskites

1. Introduction

Oxygen ion transport in ceramic oxide materials has attracted considerable interest due to the promising electrochemical applications such as solid oxide fuel cells (SOFCs). In this field, $LaGaO_3$-based perovskites are known to have superior oxygen ion conducting properties over a broad range of oxygen partial pressures.

The incorporation of divalent cation dopants to form $La_{1-x}Sr_xGa_{1-y}Mg_yO_{3-\delta}$ (often termed LSGM, where $\delta = (x+y)/2$), gives rise to highly mobile oxygen vacancies. As a consequence, the resulting ionic conductivities of LSGM at 700 °C is about four times larger than that of conventional yttria-stabilized zirconia (YSZ) electrolyte[1–3] and it is apparent that a significant decrease in the SOFC operating temperature would be an important practical advance.[4] Following the initial discovery,[1–5] numerous experimental studies have been carried out on LSGM materials, which also include the effect of transition-metal doping.[6–11] It is generally believed that doping with a transition metal cation is undesirable for the ionic conductor due to the appearance of n- or p-type conduction. However, it was found that the oxide ion conductivity was also improved by doping Co for Ga in $LaGaO_3$-based perovskites,[7] although hole conduction was detected at high oxygen partial pressures.[7,11] Nevertheless, Yamada et al.[12] demonstrated that the Co-doped LSGM (LSGMC) can be used as an electrolyte for SOFCs operating at 770 °C. The 1-kW stack they tested had a fuel electrode that consisted of a mixture of NiO and $Ce_{0.8}Sm_{0.2}O_{2-\delta}$ (SDC) and a $Sm_{0.5}Sr_{0.5}CoO_{3-\delta}$ (SSC) cathode.

LSGM materials are usually prepared by conventional solid state reactive firing,[1,2] although new powder production techniques, such as ultrasonic spray pyrolysis,[13] combustion synthesis[14] and sol–gel method[15] have been used. Tas and co-workers[16,17] have studied the preparation of LSGM powders by Pechini method, which is a versatile sol–gel method that proceeds via the formation of a polymeric resin using citric acid and ethylene glycol.[18]

However, both phase purity and microstructure of LSGM materials depend on synthetic procedure and processing and, as a matter of fact, the synthesis of a single phase per-

* Corresponding author. Tel.: +39 06 72594414; fax: +39 06 72594328.
E-mail address: polini@uniroma2.it (R. Polini).

Table 1
Nominal composition, sintering cycle, shrinkage and density of LSGM and Co-doped LSGM sintered pellets

Sample	Nominal composition	Sintering cycle	Shrinkage ($\Delta R/R_0$) (%)	Density (g/cm^3)	Theoretical density (g/cm^3)	Fractional density (%)
LSGM	$La_{0.8}Sr_{0.2}Ga_{0.8}Mg_{0.2}O_{2.8}$	1475 °C (20 h)	14.6	5.75	6.45[7,20]	89.1
LSGMC$_{10}$	$La_{0.8}Sr_{0.2}Ga_{0.8}Mg_{0.10}Co_{0.10}O_{3-\delta}$	1475 °C (20 h)	17.7	6.51	6.65[7]	97.9
LSGMC$_{8.5}$-5	$La_{0.8}Sr_{0.2}Ga_{0.8}Mg_{0.115}Co_{0.085}O_{3-\delta}$	1475 °C (5 h)	17.3	6.40	6.68[7]	95.8
LSGMC$_{8.5}$-10	$La_{0.8}Sr_{0.2}Ga_{0.8}Mg_{0.115}Co_{0.085}O_{3-\delta}$	1475 °C (10 h)	17.3	6.37		95.4
LSGMC$_{8.5}$-20	$La_{0.8}Sr_{0.2}Ga_{0.8}Mg_{0.115}Co_{0.085}O_{3-\delta}$	1475 °C (20 h)	17.7	6.43		96.3
LSGMC$_5$	$La_{0.80}Sr_{0.20}Ga_{0.80}Mg_{0.15}Co_{0.05}O_{3-\delta}$	1475 °C (20 h)	16.9	6.22	6.54[7]	95.1

ovskite is rather difficult.[13] Even sol–gel methods, which ensure the formation of polymeric precursor resins where cations are expected to be uniformly dispersed at an atomic scale, can give rise to LSGM materials containing, at the end of the preparation process, small amounts of undesired phases such as $LaSrGa_3O_7$, $LaSrGaO_4$[16] and MgO.[19] Majewski et al.[17] showed that sintering temperatures as high as 1500 °C were necessary to prepare pure $La_{0.8}Sr_{0.2}Ga_{0.8}Mg_{0.2}O_{2.8}$ ceramics by mixed oxide route or Pechini method. Schulz and Martin.[23] reported the sol–gel synthesis of pure $La_{0.8}Sr_{0.2}Ga_{0.8}Mg_{0.2}O_{2.8}$. However, to get a pure perovskite phase, they performed a very long (120 h) firing treatment at 1400 °C of the uniaxially pressed multiphase precursor, thus resembling typical conditions of time-consuming solid state reactive sintering.

Given the promising properties of Co-doped LSGM (LSGMC) electrolytes for the development of intermediate temperature (IT) SOFCs, in the present paper we continue our previous work on sol–gel synthesis of dense LSGM ceramics[19] and for the first time, in accordance to the knowledge of the authors, we describe the synthesis of LSGMC electrolytes by sol–gel method.

2. Experimental

The powders were synthesized using the following starting materials: La_2O_3 (99.9% pure, Aldrich), $SrCO_3$ (99% pure, Carlo Erba), MgO (99% pure, Carlo Erba), Co (99.9% pure, Aldrich), and a fresh solution of $Ga(NO_3)_3 \cdot xH_2O$ (99.9% pure, Aldrich). The approximate value of x in the formula of gallium nitrate was estimated by using thermogravimetric analysis (TG/DTA, Netzsch STA 409). Then a solution containing about 0.1 g/L of gallium nitrate was prepared and standardized by ICP. Before weighing, MgO and La_2O_3 were fired at 1000 °C overnight to decompose carbonate and hydroxide impurities. Stoichiometric amounts of solid powders were dissolved in $HNO_3:H_2O = 1:1$ and then the proper amount of Ga^{3+} solution was added at room temperature. Citric acid was added in the molar ratio 2:1 with respect to the total amount of cations. Heating this solution at 80–90 °C under stirring yielded a gel, in which the cations were expected to be statistically distributed in chelate complexes. The formed gel was further heated until solid foam was formed. The foam was then ground and dried at 200 °C

overnight. The obtained resin was ground, slowly heated (0.5 °C/min) to 450 °C, held at this temperature for 2 h and then heated up to 1000 °C at 10 °C/min and held at this temperature for 24 h so that all remaining organic residuals were decomposed.

The powders were ground in an agata mortar and then uniaxially pressed at 300 MPa into a 13 mm diameter cylindrical die. Pellets with 1–2 mm thickness were sintered in air at 1475 °C for 5–20 h, with a heating rate of 10 °C/min. The shrinkage of the pellets, $\Delta R/R_0$, was determined by measuring the final diameter of each sintered pellet, being 13 mm the initial green diameter (R_0). The density of the pellets was determined by Archimedes's technique.
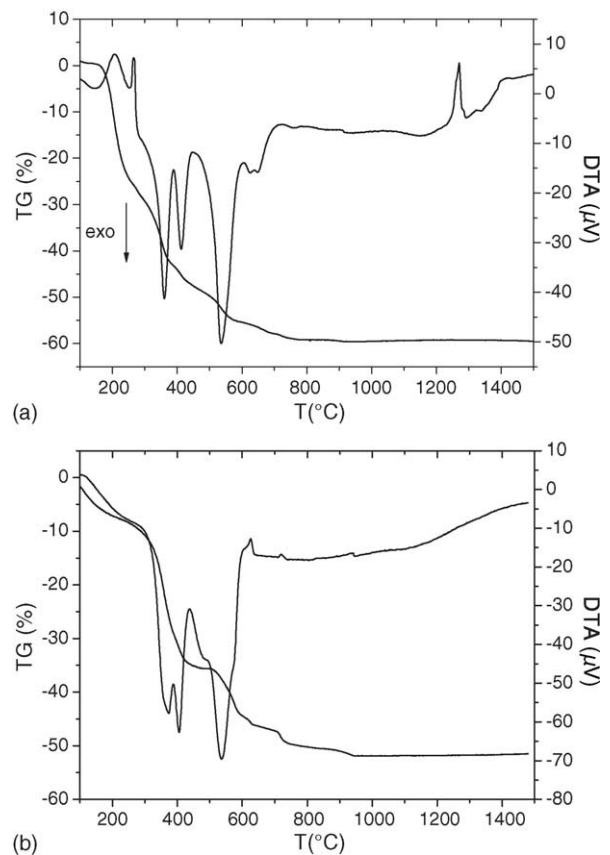

Fig. 1. TG/DTA curves of the LSGM (panel a) and LSGMC$_{8.5}$ (panel b) foams obtained by sol–gel citrate synthesis and previously dried at 200 °C overnight. The TG/DTA curves of the other powder precursors with different Co contents were similar to the one shown in panel b.

Table 1 summarizes nominal composition, sintering treatment and density of the pellets. LSGM refers to $La_{0.8}Sr_{0.2}Ga_{0.8}Mg_{0.2}O_{2.8}$ material. LSGMC$_z$ refers to doped $La_{0.8}Sr_{0.20}Ga_{0.8}Mg_{0.2-x}Co_xO_{3-\delta}$ materials, where $z = 100x$ represents the mole percent of cobalt ions in B sites of the perovskite, substituting Mg^{2+}. Three different Co levels were studied, with $x = 0.05$, 0.085 and 0.10. The LSGM material was prepared and characterized for sake of comparison.

The decomposition of the dried resins was monitored by simultaneous thermogravimetric and differential thermal analysis (TG/DTA, Netzsch STA 409) to select the proper thermal treatments to obtain the oxide powders. The analyses were carried out in air from room temperature to 1500 °C with a heating rate of 5 °C/min. Phase purity of calcined powders and of sintered pellets was determined by X-ray diffraction (XRD, Philips X'Pert Pro) at room temperature. Scans were taken with a 2θ step of 0.02° and using graphite-filtered Cu Kα radiation (40 kV, 40 mA).

The morphology of the powders as well as the microstructure of the sintered pellets was observed by field emission scanning electron microscopy (FE-SEM, Leo Supra 35). The grain size of sintered pellets was estimated by using the mean intercept method.[21] The chemical composition of the pellets was assessed by quantitative energy dispersive X-ray spectroscopy (EDS, Oxford Inca 300).

3. Results and discussion

Fig. 1 shows the TG/DTA curve of the LSGM (panel a) and of the LSGMC$_{8.5}$ (panel b) powder precursors. The TG/DTA curves of the other LSGMC precursors were quite similar to the one shown in Fig. 1b. TG curves showed a significant weight loss (>35 wt.%) due to the oxidative decomposition of organic residuals in the 200–450 °C range, accompanied by large exothermic peaks in DTA curves. At approximately 500 °C, another mass loss started, accompanied by exothermic effects, which could be attributed to the combustion of carbonaceous residuals. The rather sharp endothermic peak observed in the case of the LSGM precursor at about 1250 °C, without any associated weight loss, was attributed to solid state reactions. It is worth noting that this endothermic peak was never observed in the TG/DTA curves of LSGMC precursors.

Fig. 2 shows the SEM micrographs of LSGM and LSGMC powders obtained after the firing treatment at 1000 °C. The particle size of the powders was in the 50–300 nm range.

Fig. 3 shows the XRD patterns of LSGM and LSGMC powders. After calcination at 1000 °C (24 h) the powders were found to contain the $LaGaO_3$-based perovskite phase (JCPDS card no. 83-566) and secondary phases such as $LaSrGa_3O_7$ (237, JCPDS card no. 86-1839) and $LaSrGaO_4$ (214, JCPDS card no. 83-1004). The relative amounts of these phases were estimated by measuring the ratio, A_s/A_p, of the total integrated intensities of the most intense XRD peaks of
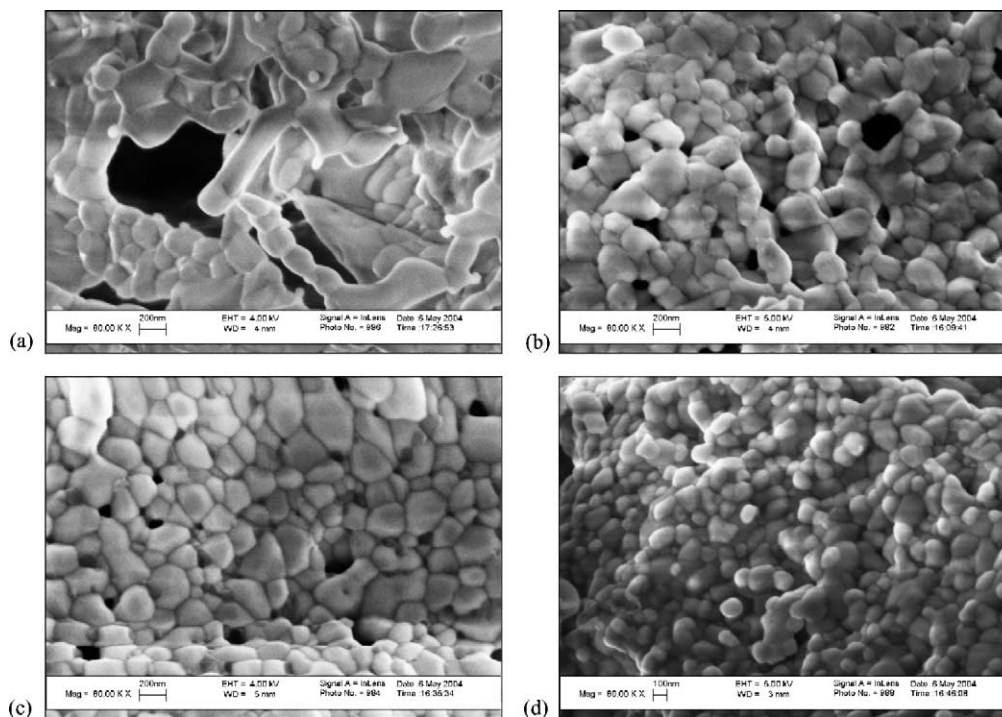

Fig. 2. SEM micrographs of different powders obtained by 24 h firing at 1000 °C: (a) LSGM, (b) LSGMC$_5$, (c) LSGMC$_{8.5}$, (d) LSGMC$_{10}$. The composition of the samples is reported in Table 1.
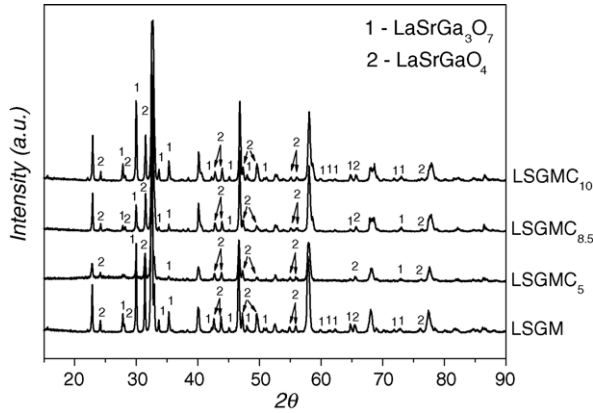
Fig. 3. XRD patterns of the powders shown in Fig. 2.

Fig. 4. XRD patterns of pellets obtained after 20 h sintering at 1475 °C of powders shown in Fig. 2.

$LaSrGa_3O_7$ and $LaSrGaO_4$ over the integrated intensity of the (1 2 1) peak of the perovskite. Table 2 reports the A_s/A_p ratios for all the powders. The $LSGMC_{8.5}$ and $LGMC_5$ powders exhibited a higher phase purity, being the A_s/A_p ratio slightly larger than 20%, while the A_s/A_p ratio for both LSGM and $LSGMC_{10}$ powders was around 40%.

In Table 1, the density of pellets obtained after powder pressing (300 MPa) and sintering at 1475 °C are reported. The data clearly showed that fractional densities larger than 95% were obtained for Co-doped LSGM pellets, while the fractional density of the LSGM pellet submitted to the same sintering cycle was lower, and around 90%. The larger sinterability of Co-doped samples cannot be ascribed to particle size effects. In fact, as shown in Fig. 2, all powders
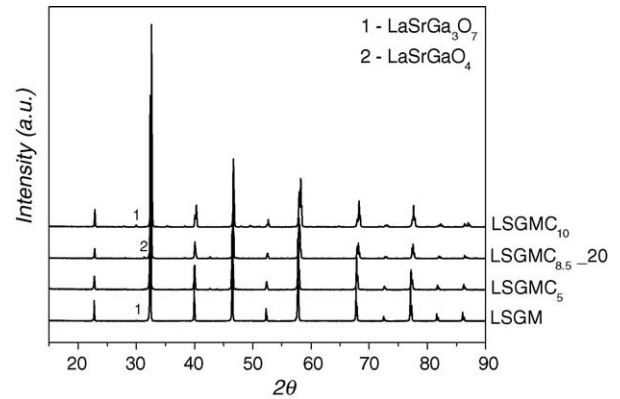
Table 2
Estimation of the amount of secondary phases in calcined powders and sintered pellets of LSGM and LSGMC materials (Table 1)

Powder	A_s/A_p (%)	Pellet	A_s/A_p (%)
LSGM	41.3	LSGM	0.82
$LSGMC_{10}$	37.4	$LSGMC_{10}$	0.94
$LSGMC_{8.5}$	20.6	$LSGMC_{8.5}\_5$	0.93
		$LSGMC_{8.5}\_10$	0.40
		$LSGMC_{8.5}\_20$	0.94
$LSGMC_5$	24.3	$LSGMC_5$	Undetectable

The A_s/A_p values represent the ratio of the total integrated intensities of the most intense XRD peaks of secondary phases over the integrated intensity of the (1 2 1) peak of the perovskite phase.
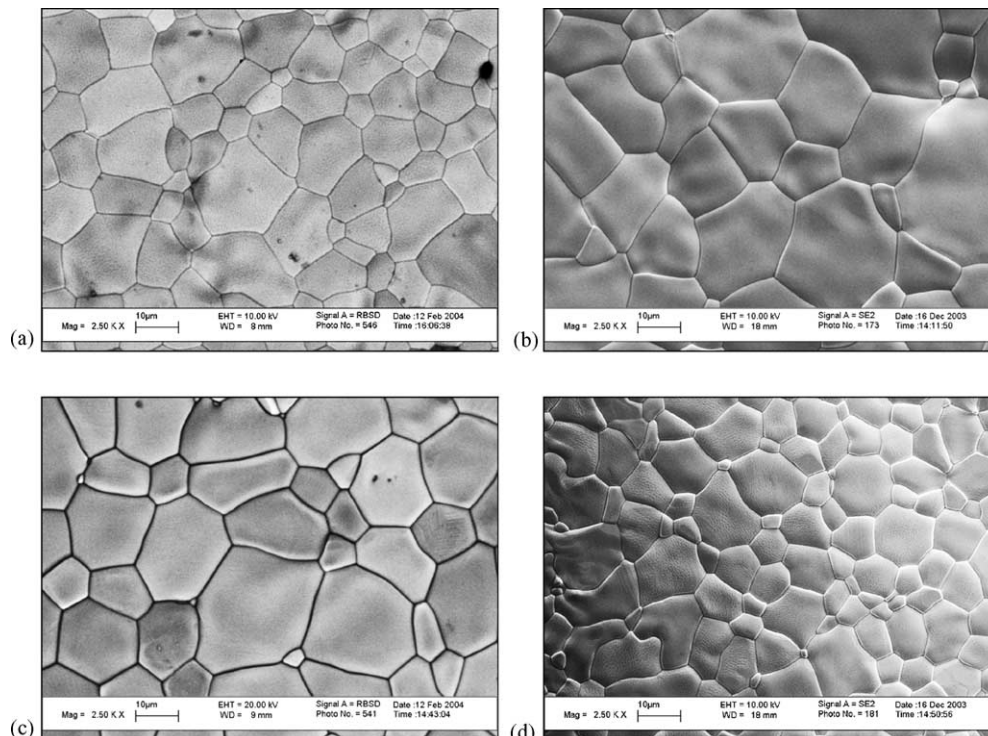

Fig. 5. SEM micrographs of sintered pellets obtained after 20 h sintering at 1475 °C: (a) LSGM, (b) $LSGMC_5$, (c) $LSGMC_{8.5}$, (d) $LSGMC_{10}$.

Table 3
Nominal and experimental stoichiometric indexes of Co-doped sintered pellets (Table 1)

Element	La	Sr	Ga	Mg	Co
LSGMC$_5$					
Nominal stoichiometric index	0.80	0.20	0.80	0.15	0.05
Experimental stoichiometric index	0.84 ± 0.02	0.16 ± 0.02	0.83 ± 0.02	0.13 ± 0.02	0.04 ± 0.01
LSGMC$_{8.5}$_20					
Nominal stoichiometric index	0.80	0.20	0.80	0.115	0.085
Experimental stoichiometric index	0.87 ± 0.04	0.13 ± 0.03	0.86 ± 0.02	0.065 ± 0.02	0.07 ± 0.01
LSGMC$_{8.5}$_10					
Nominal stoichiometric index	0.80	0.20	0.80	0.115	0.085
Experimental stoichiometric index	0.83 ± 0.02	0.17 ± 0.02	0.82 ± 0.04	0.09 ± 0.02	0.08 ± 0.01
LSGMC$_{8.5}$_5					
Nominal stoichiometric index	0.80	0.20	0.80	0.115	0.085
Experimental stoichiometric index	0.82 ± 0.01	0.18 ± 0.02	0.83 ± 0.02	0.08 ± 0.01	0.09 ± 0.004
LSGMC$_{10}$					
Nominal stoichiometric index	0.80	0.20	0.80	0.10	0.10
Experimental stoichiometric index	0.85 ± 0.01	0.14 ± 0.02	0.81 ± 0.01	0.095 ± 0.01	0.095 ± 0.01

The experimental values were determined by quantitative EDS analyses.

had particles whose sizes were few hundreds of nanometer. Therefore, we infer that Co-doping enhanced oxygen ion mobility and reduced the dopant-vacancy binding energy,[22] thus favouring the overall ion mobility at high temperatures.

Fig. 4 shows the XRD patterns of the pellets after 20 h sintering at 1475 °C. The data clearly showed that the relative amounts of secondary phases considerably decreased after sintering. In fact, in all samples the A_s/A_p ratio was lower than 1%. In particular, no secondary phases could be detected by XRD in the case of LSGMC$_5$ sintered pellet, thus indicating that high purity Co-doped LSGM electrolytes can be prepared by sol–gel citrate method. The decrease of Sr-containing secondary phases confirmed our previous findings.[19] This might be attributed to decomposition of 214 and 237 phases and subsequent solid state reactions occurring at the sintering temperature, which were promoted by the intimate contact of the particles in pressed compact. The effect of sintering time on both fractional density (Table 1) and phase purity (Table 2) was studied for the LSGMC$_{8.5}$ samples. The results pointed out that dense LSGMC$_{8.5}$ ceramics with very high phase purity was obtained after 5 h sintering.

Fig. 5 shows the SEM micrographs of LSGM and Co-doped LSGM pellets after 20 h sintering. The average grain size of pellets LSGMC$_5$ and LSGMC$_{8.5}$ was in the 11–19 μm range. To check the chemical composition and homogeneity of Co-doped sintered pellets, we performed spot EDS microanalyses of several grains for each LSGMC sample. The results of the quantitative EDS analyses are reported in Table 3 and showed a very good agreement between the experimental stoichiometric indexes and the nominal ones.

4. Conclusions

The sol–gel citrate method is clearly suitable for preparing dense and high purity Co-doped LSGM (LSGMC) sintered pellets with controlled composition. Sintering cycles performed at 1475 °C and as short as 5 h were sufficient to obtain pellets with fractional density larger than 95% and with less than 1% secondary phases (LaSrGa$_3$O$_7$ and LaSrGaO$_4$). No Co-containing phases were detected neither in the powder nor in the sintered pellets and this fact suggested that Co^{n+} ions were easily incorporated in the B sites of the perovskite lattice. The data clearly showed the feasibility of sol–gel methods to produce Co-doped LSGM perovskite type oxides, which represent promising solid electrolytes for IT-SOFCs.

References

1. Ishihara, T., Matsuda, H. and Takita, Y., Doped LaGaO$_3$ perovskite type oxide as a new oxide ionic conductor. *J. Am. Chem. Soc.*, 1994, **116**, 3801–3803.
2. Huang, P. and Petric, A., Superior oxygen ion conductivity of lanthanum gallate doped with strontium and magnesium. *J. Electrochem. Soc.*, 1996, **143**, 1644–1648.
3. Huang, K., Feng, M. and Goodenough, J. B., Sol–gel synthesis of a new oxide-ion conductor Sr- and Mg-doped LaGaO$_3$ perovskite. *J. Am. Ceram. Soc.*, 1996, **79**, 1100–1104.
4. Maric, R., Ohara, S., Fukui, T., Yoshida, H., Nishimura, M., Inagaki, T. *et al.*, Solid oxide fuel cells with doped lanthanum gallate electrolyte and LaSrCoO$_3$ cathode, and Ni-samaria-doped ceria cermet anode. *J. Electrochem. Soc.*, 1999, **146**, 2006–2010.
5. Ishihara, T., Matsuda, H. and Takita, Y., Effect of rare earth cations doped for La site on the oxide ionic conductivity of LaGO$_3$-based perovskite type oxide. *Solid State Ionics*, 1995, **79**, 147–151.
6. Ishihara, T., Akbay, T., Furutani, H. and Takita, Y., Improved oxide ion conductivity of Co doped La$_{0.8}$Sr$_{0.2}$Ga$_{0.8}$Mg$_{0.2}$ perovskite type oxide. *Solid State Ionics*, 1998, **113–115**, 585–591.
7. Ishihara, T., Furutani, H., Honda, M., Yamada, T., Shibayama, T., Akbay, T. *et al.*, Improved oxide ion conductivity in La$_{0.8}$Sr$_{0.2}$Ga$_{0.8}$Mg$_{0.2}$ by doping Co. *Chem. Mater.*, 1999, **11**, 2081–2088.
8. Trofimenko, N. and Ullmann, H., Transition metal doped lanthanum gallates. *Solid State Ionics*, 1999, **118**, 215–227.
9. Trofimenko, N. and Ullmann, H., Co-doped LSGM: composition–structure–conductivity relations. *Solid State Ionics*, 1999, **124**, 263–270.

10. Ishihara, T., Shibayama, T., Honda, M., Nishiguchi, H. and Tacita, Y., Intermediate temperature solid oxide fuel cells using $LaGaO_3$ electrolyte: II. Improvement of oxide ion conductivity and power density by doping Fe for Ga site of $LaGaO_3$. *J. Electrochem. Soc.*, 2000, **147**, 1332–1337.

11. Kharton, V. V., Yaremchenko, A. A., Viskup, A. P., Mather, G. C., Naumovich, E. N. and Marques, F. M. B., Synthesis, physicochemical characterization and ionic conductivity of $LaGa_{0.4}Mg_{0.2}M_{0.4}O_{3−\delta}$ (M = Cr, Mn, Fe, Co). *J. Electroceram.*, 2001, **7**, 57–66.

12. Yamada, T., Chitose, N., Akikusa, J., Murakami, N., Akbay, T., Miyazawa, T. *et al.*, Development of intermediate-temperature SOFC module using doped lanthanum gallate. In *Proceedings of the Eighth International Symposium on Solid Oxide Fuel Cells (SOFC-VIII)*, ed. C. Singhal and M. Dokiya. The Electrochemical Society Inc., Pennington, NJ, USA, 2003, pp. 113–118.

13. Djurado, E. and Labeau, M., Second phases in doped lanthanum gallate perovskites. *J. Eur. Ceram. Soc.*, 1998, **18**, 1397–1404.

14. Stevenson, J. W., Armstrong, T. R., McCready, D. E., Pederson, L. R. and Weber, W. J., Processing and electrical properties of alkaline earth-doped lanthanum gallate. *J. Electrochem. Soc.*, 1997, **144**, 3613–3620.

15. Huang, K. and Goodenough, J. B., Wet chemical synthesis of Sr- and Mg-doped $LaGaO_3$, a perovskite-type oxide-ion conductor. *J. Sol. State Chem.*, 1998, **136**, 274–283.

16. Tas, A. C., Majewski, P. and Aldinger, F., Chemical preparation of pure and strontium- and/or magnesium-doped lanthanum gallate powders. *J. Am. Ceram. Soc.*, 2000, **83**, 2954–2960.

17. Majewski, P., Rozumek, M., Tas, C. A. and Aldinger, F., Processing of (La,Sr)(Ga,Mg)O_3 solid electrolyte. *J. Electroceram.*, 2002, **8**, 65–73.

18. M. Pechini, U.S. Patent No. 3 330 697 (11 July 1967).

19. Polini, R., Pamio, A. and Traversa, E., Effect of synthetic route on sintering behaviour, phase purity and conductivity of Sr- and Mg-doped $LaGaO_3$ perovskites. *J. Eur. Ceram. Soc.*, 2004, **24**, 1365–1370.

20. Zha, S., Xia, C., Fang, X., Wang, H., Peng, D. and Meng, G., Processing and electrical properties of doped-$LaGaO_3$ by gelcasting. *Ceram. Int.*, 2001, **27**, 649–654.

21. German, R. M., *Sintering Theory and Practice*. John Wiley & Sons Inc., New York, USA, 1996.

22. Saiful Islam, M. and Andrew Davies, R., Atomistic study of dopant site-selectivity and defect association in the lanthanum gallate perovskite. *J. Mater. Chem.*, 2004, **14**, 86–93.

23. Schulz, O. and Martin, M., *Solid State Ionics*, 2000, **135**, 549–555.